STRUCTURAL SOURCE IDENTIFICATION FROM ACOUSTIC MEASUREMENTS USING AN ENERGETIC APPROACH

A. Samet **M. A. Ben Souf***

Laboratoire de Tribologie et Dynamique des Systèmes (LTDS)
Ecole Centrale Lyon
Lyon, France

Mechanics, Modelling and Production Laboratory (LA2MP)
Ecole Nationale d'Ingénieurs de Sfax
Sfax, Tunisie

O. Bareille **M. N. Ichchou**

Laboratoire de Tribologie et Dynamique des Systèmes (LTDS)
Ecole Centrale Lyon
Lyon, France

T. Fakhfakh **M. Haddar**

Mechanics, Modelling and Production Laboratory (LA2MP)
Ecole Nationale d'Ingénieurs de Sfax
Sfax, Tunisie

ABSTRACT

An inverse energy method for the identification of the structural force in high frequency ranges from radiated noise measurements is presented in this paper. The radiation of acoustic energy of the structure coupled to an acoustic cavity is treated using an energetic method called the simplified energy method. The main novelty of this paper consists in using the same energy method to solve inverse structural problem. It consists of localization and quantification of the vibration source through the knowledge of acoustic energy density. Numerical test cases with different measurement points are used for validation purpose. The numerical results show that the proposed method has an excellent performance in detecting the structural force with a few acoustical measurements.

Keywords: Source localization, Inverse simplified energy method, Inverse problem, High frequencies.

1. INTRODUCTION

The identification of excitation sources from operating measurement is a recent interesting scientific domain which has been treated by several researchers. In the structural or civil engineering, structures modeled with plate have important applications. Indeed, the dynamic behavior of plate coupled with a fluid has been investigated in many studies [1-4]. Thus, the localization and estimation of structural force is essential.

The identification of mechanical and acoustic sources exciting structures and cavities by direct estimation based on the measurement of some accessible quantities such as accelerations, velocities, displacements and acoustic pressure is extremely difficult. For this reason, an indirect sources measurement method to estimate the excitation sources is often employed to solve the problem.

Many researches have been used in the past decades, in order to identify the vibration load applied in the structures through a direct measurement data in the low frequency ranges. Among these approaches, the force analysis technique (FAT), also known as the RIFF technique, which was introduced years ago by Pezerat *et al.* [5, 6]. It was developed to identify the mechanical force applied to a structure through the knowledge of the displacement field measurement. Several studies have been developed with the FAT method so as to detect the force [7], moment for simple structures such as beam [7], plates [8] and shells [9], where the motion equation is analytically known.

Other methods are also used to provide an accurate result, such as the near field acoustic holography (NHA). This method was first used by Maynard *et al.* [10, 11] to identify the input sources. The idea consists in defining the acoustic source through the measurement of sound pressure field on a hologram surrounding the source.

* Corresponding author (bensouf.mohamedamine@gmail.com)

DOI : 10.1017/jmech.2017.24
Copyright © 2017 The Society of Theoretical and Applied Mechanics
https://doi.org/10.1017/jmech.2017.24 Published online by Cambridge University Press

Recently, a hybridization between the FAT and NHA methods has been used to identify vibration sources from radiated noise measurements [12]. Other inverse method, so called finite difference schemes, has been used recently by Djamaa *et al.* [13] to localize the sound source using the measured dynamic response of a cylinder. The inverse FEM and BEM were also used by authors to estimate the vibration sources in the low frequency ranges [14-17]. However, these techniques require finer meshes and the calculations are too heavy when the frequency increases, precisely at high frequency range.

It should be noticed that the most of the proposed investigations in the literature were limited on the low frequency band, which is characterized by a week model overlap and a dominant resonant behavior. Generally, in the high frequency band, the uses of these kinds of inverse techniques can be time consuming and require very high calculation costs. To solve the limitation of these methods, energy methods are often used. They provide an efficient tool for the evaluation of averages energy in a high frequency range. Among these approaches, the statical energy analysis (SEA) [18] which consists in subdividing the system into connected subsystems, and assuming that the energy fields are diffused, in order to calculate the average value of energy quantities exchanged between subsystems. Several investigations have been conducted to improve the SEA. In fact, they tried, not only to predict the energy density, but also to estimate the power flow fields and the energy distribution inside systems. Among these developments, the local energy formulation was devised by Nefske and Sang [19] and developed by Bernhard *et al*. [20, 21] and also discussed in references [22] and [23]. These improvements further lead to a simplified energy method (MES) for the medium and high frequency ranges. The direct theory formulation has been applied in various domains including beam [24], membrane and plates [25] and acoustic applications [26, 27]. Several researches were made to develop and expand this method in order to predict the structural and acoustic sources using the inverse MES method (IMES). The IMES has been first used by Chabchoub *et al*. [28] to estimate the structural force applied in plate through the measurement of the structural density field. This method was also used in acoustic cavity application [29]. The idea consists in defining the acoustic boundary source through the measurement of sound pressure field. Recently, the IMES has been developed by Samet *et al*. [30] for a complex structure modeled with many assembled plates.

The main novelty of this paper is to develop this inverse method in order to detect the structural force applied in a plate coupled with an acoustic cavity through a measurement data of the acoustic energy field. The paper is organized as follows: Section 2 deals with the inverse formulation of the MES method. In addition, details on the calculation of energy field is exhibited. Then, some numerical cases are presented and validated in Section 3.

2. THE INVERSE SIMPLIFIED ENERGY METHOD (IMES)

2.1 Assumptions

The simplified energy method is a vibro-acoustic method developed for the purpose to predict the energy density distribution for structural acoustic problem in high frequency ranges. This method is based on a description of two local energy quantities. The first is the energy density W defined as a sum of the kinetic and potential energy densities, and the second $\vec{I}$ is the energy flow inside the system. The energy flow balance of a system can be written as follows:

$$\Pi^{in} = \Pi^{diss} + \vec{\nabla}.\vec{I} \tag{1}$$

where Π^{diss} is the local dissipated power density, $\vec{\nabla}$ is the gradient operator and Π^{in} is the local input density. MES adopts the same damping model as that in SEA. It has been discussed in the literature [18] and can be expressed as follows:

$$\Pi^{diss} = \eta\omega W \tag{2}$$

where ω is the circular frequency and η the damping factor. The propagative waves of the simplified energy method are characterized by a simple equation depending on the energy density W, energy flow $\vec{I}$ and group velocity c_g such that [31]:

$$\vec{I} = c_g W\vec{n} \tag{3}$$

This expression is valid for undamped system and in the far field for outing traveler waves.

2.2 Energy Fields Formulation

In the following, the derivation of the MES formula is done considering a *nD* space. Thus, in our case of plate coupled with acoustic cavity, the following equations will be applied with $n = 2$ for plate and $n = 3$ for acoustic cavity. Considering a symmetrical wave field and Eqs. (1), (3), the MES approach [23] leads to the following relation:

$$\frac{1}{r^{n-1}}\frac{\partial}{\partial r}(r^{n-1}\vec{I}) + \eta\omega W\vec{n} = 0 \tag{4}$$

This equation can be rewritten considering only W field:

$$\frac{1}{r^{n-1}}\frac{\partial}{\partial r}(r^{n-1}W) + \frac{\eta\omega}{c_g}W = 0 \tag{5}$$

The solutions, in terms of energy density and active intensity, are expressed by G and $\vec{H}$ respectively:

$$G(S,M) = \frac{1}{c_g}\frac{e^{-\left(\frac{\eta\omega}{c_g}\right)r}}{\gamma_0 r^{n-1}}, \qquad \vec{H}(S,M) = \frac{e^{-\left(\frac{\eta\omega}{c_g}\right)r}}{\gamma_0 r^{n-1}}\vec{u}_{SM} \tag{6}$$

where $r = \| \overrightarrow{SM} \|$ represents the distance between the source S and the measurement point M, $\vec{u}_{SM}$ is the unit vector from M to S and γ_0 is the solid angle of considered space (2 in dimension 1, 2π in dimension 2 and 4π in dimension 3).

https://doi.org/10.1017/jmech.2017.24 Published online by Cambridge University Press

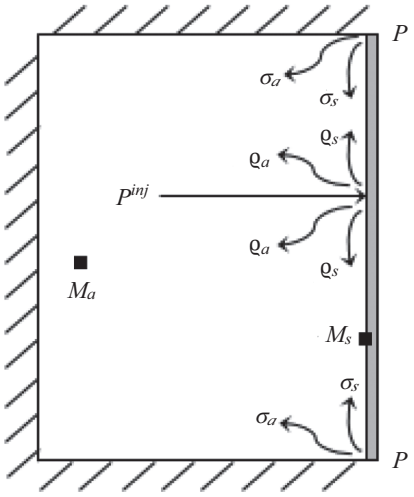


Fig. 1 System decomposition.

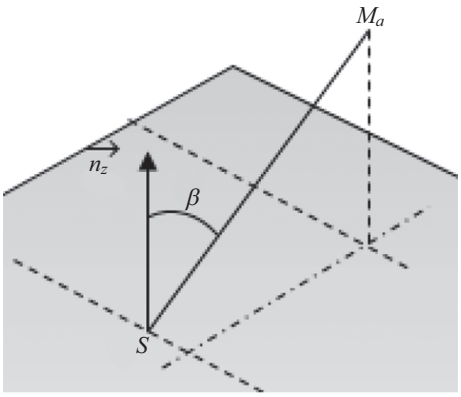


Fig. 2 Radiation of excitation point.

2.3 Systems Decomposition

Consider a clamped edge plate excited by a punctual force F, coupled with an acoustic cavity. For the purpose to predict the structural and acoustic energy fields, these fields are devised into several waves of the type described above. To simplify the problem, it is supposed that the structural plate may be seen as rigid for acoustical waves, which means that the acoustic power transmitted to the plate is neglected, which corresponds to a light fluid hypothesis.

The energy W_s on the structure is defined as the sum of the primary source ϱ_s (direct field) coming from the excitation point S, and the fictitious sources σ_s coming from the boundary P of the structure as shown in Fig. 1. Hence, the structural energy W_s at any point M_s can be written as follows:

$$W_s(M_s)=\int_{\Omega_s}\varrho_s(S)G_s(S,M_s)dS+\int_{\partial\Omega_s}\sigma_s(P)\vec{u}_{SM}.\vec{n}_P G_s(P,M_s)dP \tag{7}$$

The acoustical energy W_a radiated from the structure is described as follows. For supersonic waves, the radiation of the acoustical power is located at the excitation points S and structure boundaries P. In addition, according to the assumption that propagative waves are uncorrelated, the acoustical energy W_a at any point M_a inside the cavity is the sum of energy radiated from the excitation sources W_a^{exci} and energy W_a^{edge} radiated from the structure extremity,

$$W_a(M_a)=W_a^{exci}(M_a)+W_a^{edge}(M_a) \tag{8}$$

where

$$W_a^{exci}(M_a)=\int_{\Omega_s}\varrho_s(s,\vec{U}_{SM_a})G_a(S,M_a)dS \tag{9}$$

and

$$W_a^{edge}(M_a)=\int_{\partial\Omega_s}\varrho_s(P,\vec{U}_{PM_a})G_a(P,M_a)dP \tag{10}$$

In order to obtain the structural and acoustical energy density, the source magnitudes ϱ_a, ϱ_s, σ_a, and σ_s, are now solved. The complete system is then detailed in the next section.

2.4 Canonical Problem

2.4.1 Excitation Radiation

The objective of the following canonical problem is to calculate the power balance at the excitation point of a plate coupled to a fluid (notations are defined in Fig. 2). For a punctual excitation with the force F or moment M, displacement and pressure are expressed as functions of impedance Y, with the following Hankel transforms:

$$u(r)=\frac{1}{4\pi}\int_{-\infty}^{+\infty}Y(\gamma)H_0^1(\gamma r)\gamma d\gamma \tag{11}$$

$$p(r,z)=\frac{1}{4\pi}\int_{-\infty}^{+\infty}\rho_a\omega^2\frac{Y(\gamma)}{(k_a^2-\gamma^2)^{1/2}}H_0^1(\gamma r)\gamma e^{-j(k_a^2-\gamma^2)^{1/2}z}d\gamma \tag{12}$$

wherein z is the coordinate normal to the structure, $k_a=\dfrac{\omega}{c_a}$ is the acoustic wave number, ω is the angular frequency and Y is the ratio of a displacement to a force expressed as:

$$Y(\gamma)=\frac{(F-j\gamma M)(k_a^2-\gamma^2)^{1/2}}{D(\gamma^4-k_s^4)(k_a^2-\gamma^2)^{1/2}-j\rho_a\omega^2} \tag{13}$$

The structural power is calculated by expressing the structure field carried by propagating traveling waves. Using the asymptotic expression of Hankel function, the structural power is written as follows:

$$P^{struc}=\frac{\omega(|F|^2+|k_sM|^2)}{16Dk_s^2}\left|1-j\frac{\rho_a\omega^2}{4D}k_s^{-2}(k_a^2-k_s^2)^{-3/2}\right|^{-2} \tag{14}$$

Where $k_s=(\rho_s h\omega^2/D)^{1/4}$ the structural wave number, h the thickness of the plate and $D=Eh^3/12(1+\nu^2)$ the plate's stiffness.

https://doi.org/10.1017/jmech.2017.24 Published online by Cambridge University Press

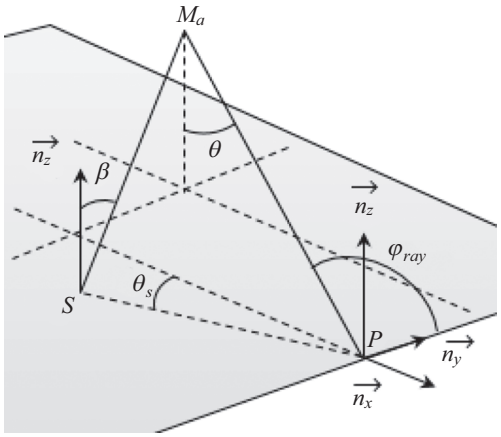


Fig. 3 Reflection in the edge; the notations.

The total power supplied to the system is the sum of the power injected into the structure (Eq. (14)) and the radiated power corresponding to the integral of the power flow diffracted on the hemisphere surrounding the excitation point: $P^{inj} = P^{struc} + P^{ray}$ with P^{ray} defined by

$$P^{ray}(\beta) = \Gamma_{exci}(\beta) P^{inj} \tag{15}$$

where

$$\Gamma_{exci}(\beta) = \frac{\rho_s \omega k_a}{4\pi^2 P^{inj}} |Y(k_a \sin(\beta)|^2 \tag{16}$$

and β is the angle with the normal of the plate.

2.4.2 Edge Radiation

The canonical problem objective is to calculate the power balance in the extremity of plate coupled with an acoustic middle (the notations are defined in Fig. 3): Starting from the displacement field due to a plane flexion wave, incident with an angle θ_s on the edge of a clamped plate, we seek to determine the intensity of the radiated power. The structure is placed in $x < 0$, and the boundary at $x = 0$. The displacement field is defined in $x > 0$ by: $u(x,y) = u(x)e^{-jk_s \sin(\theta_s)y}$ with $u(x) = u_i(e^{-jk_s \cos(\theta_s)x} + re^{jk_s \cos(\theta_s)x} + r_e e^{k_s \cos(\theta_s)x})$ including the incident term and the reflected terms propagative and evanescent. For a clamped plate the r and r_e values are: $r = -1$ and $r_e = 0$ [32].

The fluid is now introduced by considering the acoustic pressure in the form $p(x,y,z) = p(x,z)e^{-jk_s \sin(\theta_s)y}$. The pressure $p_2(x, z)$ is defined by:

$$p_2(x,z) = p(x,z) - \frac{j\rho_a \omega^2}{\sqrt{(k_a^2 - k_s^2)}} e^{-j(k_s x + (k_a^2 - k_s^2)^{1/2} z)} \tag{17}$$

where the second term corresponds to the pressure that would radiate from the incident structural wave when it propagated on x direction. Basing now on the following Helmholtz equation:

$$(\Delta + k_a^2) p = 0 \tag{18}$$

We demonstrated that the pressure p_2 satisfies the following equation:

$$\frac{\partial^2 p_2}{\partial x^2} + \frac{\partial^2 p_2}{\partial z^2} + K^2 p_2 = 0 \quad \text{with} \quad K^2(\theta_s) = k_a^2 - k_s^2 \sin^2(\theta_s) \tag{19}$$

and coupling conditions:

$$\begin{aligned} &\frac{\partial p_2}{\partial_z}(x, z=0) = \rho_a \omega^2 u_r(x) \quad x < 0; \\ &\frac{\partial p_2}{\partial z}(x, z=0) = -\rho_a \omega^2 u_i(x) \quad x > 0 \end{aligned} \tag{20}$$

The average spatial Fourier transforms on x of pressure and displacement are written as follows:

$$\begin{aligned} P_2^+(\gamma, z) &= \frac{1}{2\pi} \int_0^{+\infty} p_2(x,z) e^{j\gamma x} dx; \\ P_2^-(\gamma, z) &= \frac{1}{2\pi} \int_{-\infty}^{0} p_2(x,z) e^{j\gamma x} dx \end{aligned} \tag{21}$$

$$\begin{aligned} U_i(\gamma) &= \frac{1}{2\pi} \int_0^{+\infty} U_i(x,z) e^{j\gamma x} dx; \\ U_r(\gamma) &= \frac{1}{2\pi} \int_{-\infty}^{0} U_r(\gamma)(x,z) e^{j\gamma x} dx \end{aligned} \tag{22}$$

with $P_2 = P_2^+ + P_2^-$ and $U = U_r - U_i$. Basing now on equation (19), the pressure is written as follows:

$$p_2(x,z) = p_2(\gamma, 0) e^{-j(K^2 - \gamma^2)^{1/2} z} \tag{23}$$

and the coupled equation (20) is written as follows:

$$\begin{aligned} P_2^+(\gamma, 0) &= -j\rho_a \omega^2 \frac{U_i(\gamma)}{(K^2 - \gamma^2)^{1/2}}; \\ P_2^-(\gamma, 0) &= j\rho_a \omega^2 \frac{U_r(\gamma)}{(K^2 - \gamma^2)^{1/2}} \end{aligned} \tag{24}$$

The Fourier transform of p_2 is then:

$$\begin{aligned} p_2(\gamma, 0) = \frac{j\rho_a \omega^2}{(\gamma - K)^{1/2}} \Bigg[&\frac{1}{(\gamma + k_s \cos(\theta_s))(k_s \cos(\theta_s) - K)^{\frac{1}{2}}} \\ &+ \frac{jr}{(\gamma - k_s \cos(\theta_s))(k_s \cos(\theta_s) + K)^{\frac{1}{2}}} \\ &+ \frac{jr_e}{(\gamma - k_s \cos(\theta_s))(jk_s \cos(\theta_s) + K)^{\frac{1}{2}}} \Bigg] \end{aligned}$$

Where θ represents the angle between the normal direction to the plate and the directional radiation and φ^{ray} the spherical angle around the edge line. The specific intensity in (θ, φ^{ray}) direction is expressed in terms of the incident structural flux $\vec{I_s}$ as follows:

$$p_{ray}(\theta, \varphi^{ray}) = \Gamma_{bord}(\theta_s, \theta) \delta(\varphi - \varphi_{ray}(\theta_s)) I_s \quad \text{with}$$

https://doi.org/10.1017/jmech.2017.24 Published online by Cambridge University Press

$$\Gamma_{bord}(\theta_s,\theta)=\frac{4\pi}{k_a}\frac{|P_2(K\sin(\theta),0|^2|K\sin(\theta)|^2}{\Re_e(D(k_s^3+k_s^2k_s^*))\cos(\theta_s)} \quad (25)$$

In order to respect the power balance, the energetic structural reflection coefficient must take into account the part of power being diffracted:

$$R_s(\theta_s)=1-\int_{-\pi/2}^{\pi/2}\Gamma_{bord}(\theta_s,\theta)d\theta \quad (26)$$

2.4.3 Supersonic Waves Radiation

The radiation of supersonic flexural wave is made as follows. Using a simple calculation of the propagative forms of the displacement and pressure for an infinite fluid loaded plate, the directional specific intensity can be expressed as follows in terms of structural power flow I_s:

$$P_{ray}(\varphi)=\Gamma_{surf}\delta(\varphi-\varphi_{rad})I_s \quad \text{with} \quad \sin(\varphi_{rad})=\frac{k_s}{k_a} \quad (27)$$

Where φ_{rad} is the angle with the normal to the plate, and Γ_{surf} denotes the surface radiation efficiency:

$$\Gamma_{surf}=\frac{\rho_a\omega}{c_s\rho_s h}(k_a^2-k_s^2)^{-1/2} \quad (28)$$

This proportional relationship shows that the fluid coupling generates a loss of energy for structural waves, with equivalent damping coefficient:

$$\eta_{rad}=c_s\Gamma_{surf}/\omega \quad (29)$$

where c_s is the group velocity of structure.

2.5 Energetic Resolution of System

The system resolution requires the calculation of the total acoustic energy density W_a.

2.5.1 Acoustic Energy Radiated from the Excitation Source

The acoustic energy density is described by the integral over the secondary sources σ_a located on the structure Ω_s:

$$W_a^{exci}(M_a)=\int_{\Omega_s}\sigma_a(s,\vec{U}_{SM_a})G_a(S,M_a)dS \quad \text{with} \quad G(S,M)=\frac{1}{c_a}\frac{e^{-\left(\frac{\eta_a\omega)}{c_a}\right)SM_a}}{\gamma_0 SM_a} \quad (30)$$

Expressing the power located in the exciting point of structural $\sigma_a(s,\vec{U}_{SM_a})$ by the following expression:

$$\sigma_a(s,\vec{U}_{SM_a})=\Gamma_{exci}(\theta_a)\gamma_0 P^{inj}(S) \quad (31)$$

The acoustic energy density is written as follows:

$$W_a^{exci}(M_a)=\int_{\Omega_s}\Gamma_{exci}(\theta_a)\gamma_0 P^{inj}(S)G_a(S,M_a)dS \quad (32)$$

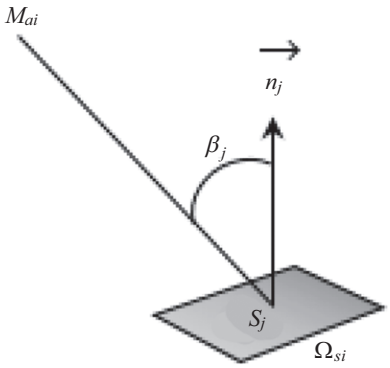


Fig. 4 Measurement point/source interaction.

2.5.2 Acoustic Eergy Rdiated from the Sructure Etremity

The energetic resolution of acoustic energy radiated in the extremity is made as follows: The structural energy density field is first solved taking into account the energetic structural reflection coefficient $R_s(\theta_s)$ coming from Eq. (26) and the power diffracted in the acoustic middle. After that, the acoustic source magnitude σ_a located in the extremity of the plate is second solved with the following expression:

$$\sigma_a(P,\vec{U}_{PM_a})=\gamma_0\frac{\Gamma_{bord}(\vec{U}_S^{ray},\theta)}{\sin(\varphi_{PM_a})}\overrightarrow{I_s}(P,\vec{U}_S^{ray}).\overrightarrow{n_p} \quad (33)$$

By introducing the acoustic source magnitude σ_a in the integral (Eq. (10)), the acoustic energy density in the extremity is written:

$$W_a^{bord}(M_a)=\int_{\partial\Omega_s}\Gamma_{bord}(\vec{U}_S^{ray},\theta)\frac{1}{c_a}\frac{e^{-\left(\frac{\eta_a\omega}{c_a}\right)PM_a}}{PM_a\sin(\varphi_{PM_a})}\overrightarrow{I_s}(P,\vec{U}_S^{ray}).\overrightarrow{n_P}dP \quad (34)$$

where the structural power flow incident $\overrightarrow{I_s}$ is defined by the following relationship:

$$\overrightarrow{I_s}(P,\vec{U}_S^{ray})=\int_{\partial\Omega_s}P^{struc}(S)\vec{H}_s(S,P)dS+\int_{\partial\Omega_s}\sigma_s(P)\vec{H}_s(P',P)dP \quad (35)$$

2.6 Inverse Formulation

This section focuses on developing an inverse MES formulation for a plate coupled with an acoustic cavity, by applying a discrete format of the energy equation Eq. (8). For this goal, we define first a matrix called $S_{a,ij}^{exci}$ presenting the interaction matrix between points source S and acoustic measurement points M_a (see Fig. 4). This matrix with dimension $(n_{M_a}^2,n_s^2)$, where n_s is the number of structural sources and n_{M_a} is the number of acoustic measurements.

$$S_{a,ij}^{exci}=\int_{\Omega_{sj}}\Gamma_{exci}(\theta_a)\gamma_0 P^{inj}(S_j)\frac{1}{c_a}\frac{e^{-\left(\frac{\eta_a\omega)}{c_a}\right)SM_{ai}}}{\gamma_0 S_j M_{ai}}dS_j \quad (36)$$

https://doi.org/10.1017/jmech.2017.24 Published online by Cambridge University Press

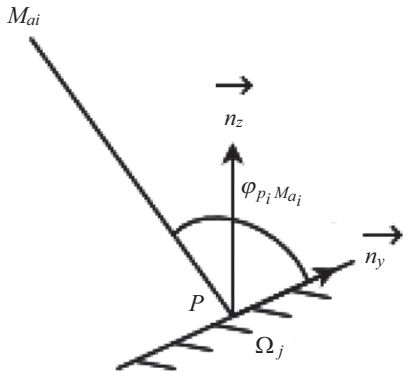


Fig. 5 Measurement point/edge element interaction.

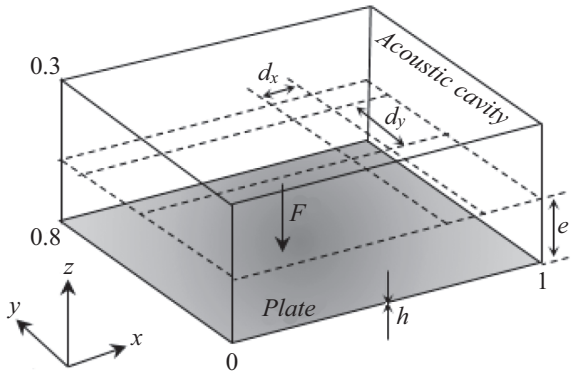


Fig. 6 Boundary conditions.

Secondly, we defined T_{ij} as the (n_P, n_P) geometric interaction matrix between n_P two edge elements. It is determined by the following formula:

$$T_{ij} = 2c_s - 2\pi R_s c_s B_{ij} \tag{37}$$

where $B_{ij} = \int_{\partial\Omega_i}\int_{\partial\Omega_j} \frac{e^{-\left(\frac{(\eta_s+\eta_{rad})\omega}{c_s}\right)P_jP_i}}{2\pi P_jP_i} \vec{u}_{P_jP_i}.\vec{n}_{P_j}\, dP_j dP_i$ and R_s is the energetic structural reflection coefficient calculated by Eq. (26).

We define a (n_P, n_S) matrix called Q_{ij} matching a geometric interaction between n_P edge elements and n_s structural sources. It is determined by the following equation:

$$Q_{ij} = \int_{\Omega_i} \frac{e^{-\left(\frac{(\eta_s+\eta_{rad})\omega}{c_s}\right)S_jP_i}}{S_jP_i} \vec{u}_{S_jP_i}.\vec{n}_{P_i}\, dP_i \tag{38}$$

Next, a matrix called V_{ij} presenting the geometric interaction between structural source points n_s and n_P edge elements is defined. This matrix with dimension (n_P, n_s^2), and it is presented as follows:

$$V_{ij} = \int_{\Omega_s} \frac{e^{-\left(\frac{(\eta_s+\eta_{rad})\omega}{c_s}\right)S_jP_i}}{2\pi S_jP_i} \vec{u}_{S_jP_i}.\vec{n}_{P_i}\, dS_i \tag{39}$$

Referring to Fig. 5 another $(n_{M_a}^2, n_P)$ matrix is defined and called Y_{ij}. This operator represents the geometric interaction between acoustic measurements points n_{M_a} and n_P edge elements. It is written as follows:

$$Y_{ij} = \int_{\Omega_i} \Gamma_{bord} \frac{1}{c_a} \frac{e^{-\left(\frac{(\eta_{sa})\omega}{c_a}\right)P_iM_{aj}}}{P_jM_{ai}\sin(\varphi_{P_iM_{aj}})} dP_i \tag{40}$$

After that, we define S_a^{edge} combined Eqs. (37-40). It is determined by the following equation:

$$S_a^{edge} = Y_{ij}.V_{ij} + Y_{ij}B_{ij}T_{ij}^{-1}Q_{ij} \tag{41}$$

For sake of clarity, the direct MES equation can then be written in the following way:

$$W_a = S_a P^{struc} \tag{42}$$

where $W_a = W_a^{exci} + W_a^{edge}$ and $S_a = S_a^{exci} + S_a^{edge}$.

The IMES formulation aims to invert the matrix formulation of Eq. (42). The structural force applied in plate can then be estimated and localized from an acoustic measurement. It is expressed as follows:

$$P^{struc} = S_a^{+} W_a \tag{43}$$

where + is the pseudo inverse, $W_a = W_a^{exci} + W_a^{edge}$ and $S_a = S_a^{exci} + S_a^{edge}$. Matrix S_a can be well-conditioned, but is often ill-conditioned, which will disturb the results. In the next parts, we studied the matrix S_a inversion influence on the numerical results.

3. NUMERICAL RESULTS

This section deals with numerical tests of different cases in order to validate the presented formulation. The presented system is a structure which consists of a plate (ρ_s = 7800 kg/m^3, υ = 0.3, E = 210 × 10^9 Pa) coupled with an acoustic cavity (ρ_s = 1.3 kg/m^3, c_s = 340 m/s). The structure is a rectangular plate, its length, width and thickness are L = 1 m, l = 0.8 m and h = 3.10^{-3} m, clamped on its borders and damped with a coefficient η_s = 1%. The acoustic cavity is undamped and with dimensions (L = 1 m, l = 0.8 m, H = 0.3 m) as shown in Fig. 6. The plate is excited with an input power P^{inj} = 1.551 W/m^2 calculated by Eq. (14), at point S given by (0.45 m, 0.45 m, 0).

Figure 7 presents the numerical simulation methodology which consists of implementing the IMES approach when using a set of acoustic density energy predicting, based in the first case on the direct simplified energy method (MES/IMES simulation), and in the second case on the finite element method (FEM/IMES simulation) modeled using COMSOL multiphysics software.

https://doi.org/10.1017/jmech.2017.24 Published online by Cambridge University Press

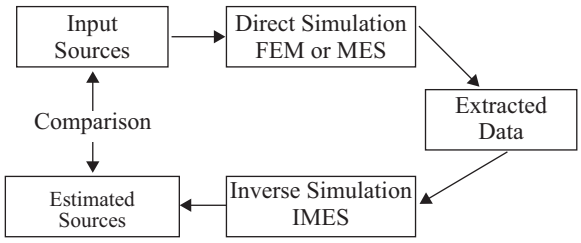


Fig. 7 Flow chart of numerical methodology.

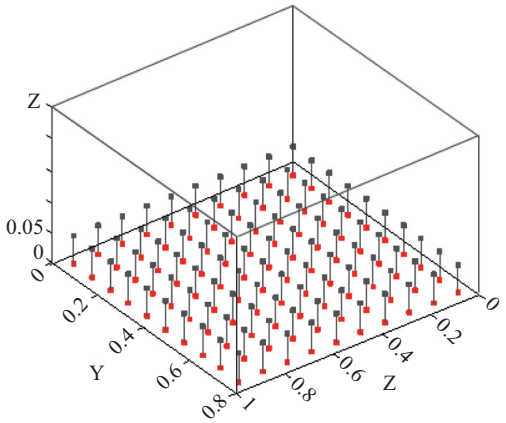


Fig. 8 Structural sources (red) and acoustic measurements (grey) repartition.

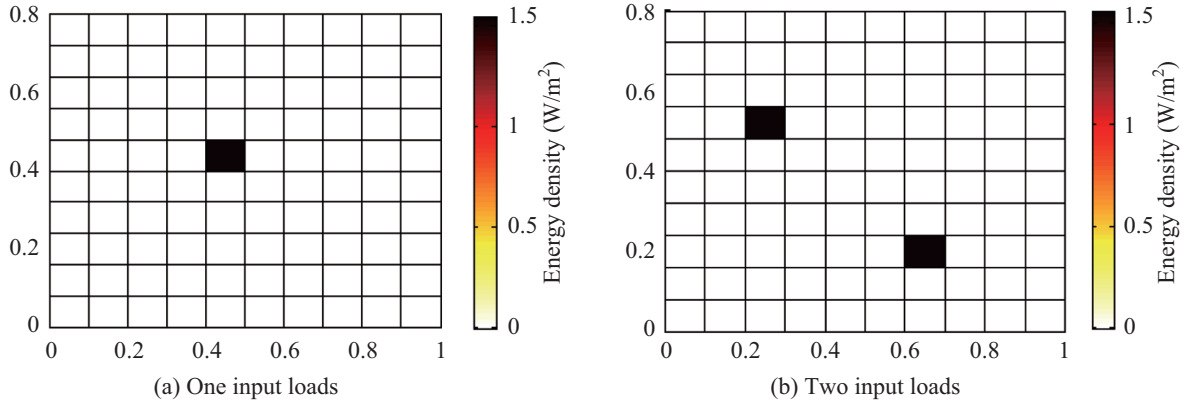


Fig. 9 MES/IMES simulation.

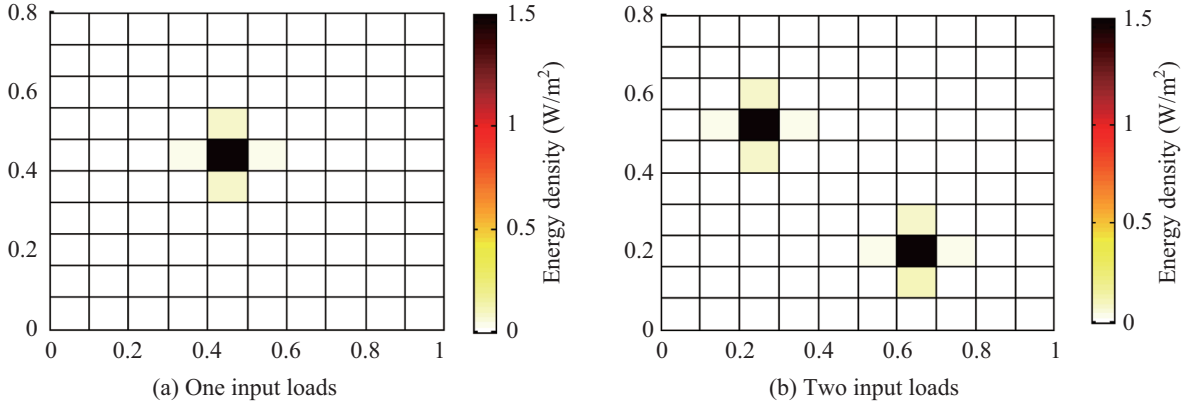


Fig. 10 FEM/IMES simulation.

3.1 Validation of the Inverse MES Formulation

An analysis presented in this section for the purpose to validate the IMES method. The displayed results are computed in an octave band with a frequency center f_c = 15 kHz, where the modal overlaps is quite high and the use of energy quantities is essential. The first step consists in determining the measurement data of the acoustic energy density field through n_{M_a} = 100 distributed on a parallel plan to the plate with a distance e = 0.05 m as shown in Fig. 8.

The second step consists in comparing the force results given by the MES/IMES and FEM/IMES simulation with the exact value of the input loads. To check the sensitivity of IMES method regarding more excitation loads, the plate is also excited in other example with two input forces P^{inj} = 1.551 W/m^2 given by (0.25 m, 0.55 m, 0) and (0.65 m, 0.25 m, 0).

It should be remembered that, the input loads were calculated using Eq. (14) and results are presented in Figs. 9 and 10. Result in Fig. 9 shows that the inversion of S_a is validated since we obtained a good estimation of

https://doi.org/10.1017/jmech.2017.24 Published online by Cambridge University Press

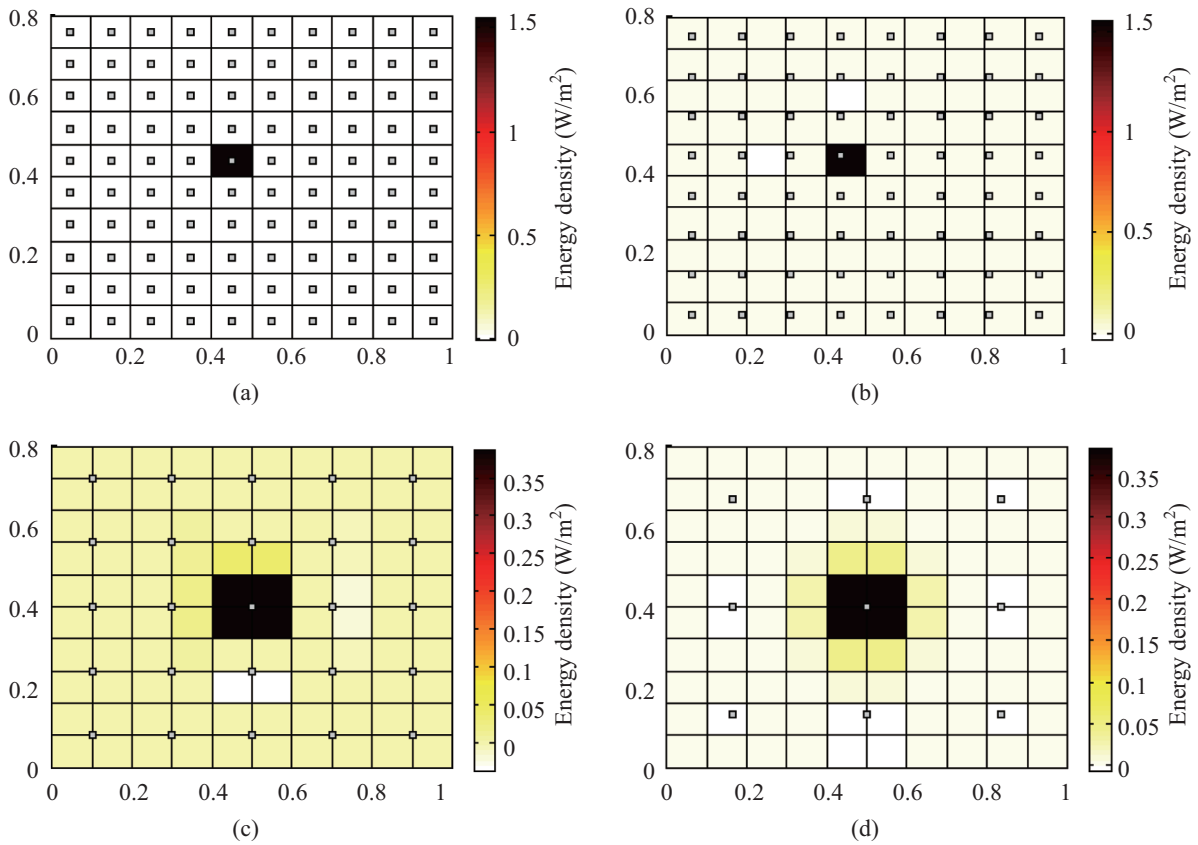


Fig. 11 MES/IMES Simulation (■ Measurement Grid) for (a) $n_{M_a} = 100$, (b) $n_{M_a} = 64$, (c) $n_{M_a} = 25$, (d) $n_{M_a} = 9$.

the location and levels for the vibratory sources. In a similar way, the FEM/IMES result was compared with the input value. Actually, the IMES calculation is processed using W_a calculated by finite element software.

Figure 10 displays the sources identification from the measured data showing that the different force positions clearly appear to be in the exact location. Furthermore, the number of load excitation does not disturb the location identification, which proves the ability of IMES method to identify the exterior excitation for different positions of the load.

3.2 Influence of Noisy Measurements

In this section, a number of numerical tests will be performed in order to show the impact of acoustic measurement point repartition in the identification of structural source. For this reason, two simulation tests were performed in order to approach to the realistic case, the first with MES/IMES simulation and the second with FEM/IMES simulation. The objective of these simulations are to analyze the influence of measurement points distribution on the detection of input load.

3.2.1 MES/IMES Simulation

The number of acoustic measurements n_{M_a} will be changed in this application. To illustrate its effect, the MES/IMES simulation was repeated while decreasing n_{M_a} and the results displayed in Fig. 11 were obtained. Let us then define the factor $\mu = n_{M_a} / n_S$ to quantify the efficiency of the method. $\mu = 1$ ($n_S = n_{M_a}$) correspond to the square matrix to invert, whereas $\mu < 1$ corresponds to a few number of measurements compared to the number of structural sources n_S. It appears that by increasing the measurements points n_{M_a} spread over each plate corresponding to $n_{M_a} = 9$ ($\mu = 0.09$), $n_{M_a} = 25$ ($\mu = 0.25$), $n_{M_a} = 64$ ($\mu = 0.64$) and $n_{M_a} = 100$ ($\mu = 1$) respectively, the source is well detected and the difference on the input power has been decreased.

For instance, the source input power is equal to 0.3805 W/m^2 for $n_{M_a} = 9$, 0.3879 W/m^2 for $n_{M_a} = 25$, 1.5503 W/m^2 for $n_{M_a} = 64$ and 1.5514 W/m^2 for $n_{M_a} = 100$, yet it should equal to 1.551 W/m^2. Therefore, the correct result of the input power is achieved for higher n_{M_a} values. To illustrate the quantification sensitivity Q_T (Fig. 12(a)) and the location sensitivity L_T (Fig. 12(b)), these terms given by the following equation were used:

$$Q_T = \sqrt{\frac{(P^{source} - P^{exact})^2}{(P^{exact})^2}}; \quad L_T = \frac{\sum_{i=1}^{N} (P^i - P^i_{exact})^2}{N} \tag{44}$$

where P^i_{exact} and P^i are respectively the i component of

https://doi.org/10.1017/jmech.2017.24 Published online by Cambridge University Press

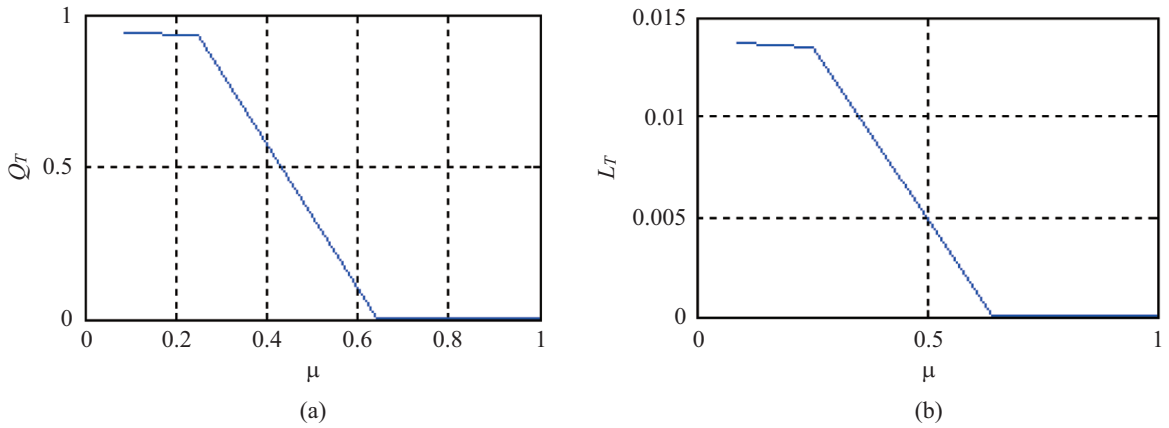


Fig. 12 Quantification (a) and location (b) terms of precision evolution as function of μ.

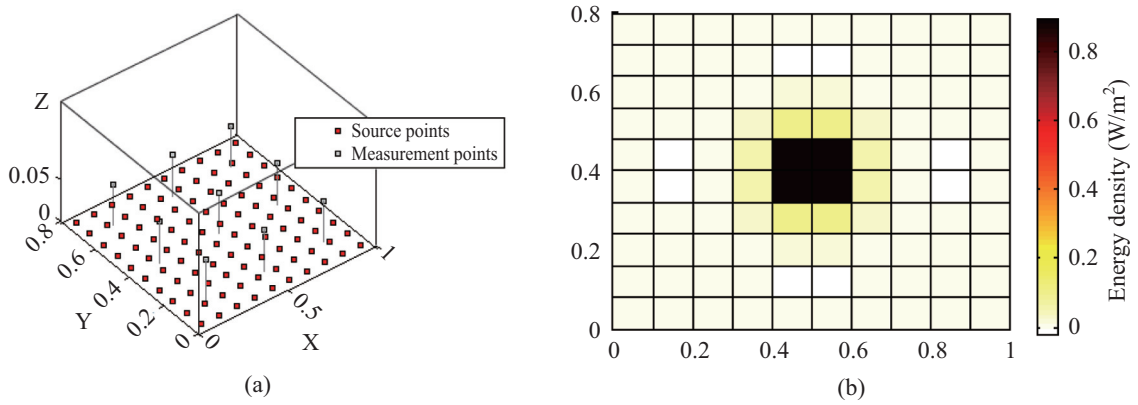


Fig. 13 FEM/IMES Simulation for $d_x = 0.33$ m and $d_y = 0.26$ m.

the exact input power vector and the i component of the estimated power vector. It is clear that the values of Q_T and L_T increase when the value of $\mu = n_{M_a} / n_S$ decreases, which means that the IMES is validated with a good accuracy for the higher n_{M_a} values. It is observed that good results are obtained from μ = 1, which corresponds to $n_{M_a} = n_S$.

As a conclusion, the IMES formulation tends to estimate the injected power when the numbers of measurement data obtained with the direct MES formulation are higher. Let us show in the next section the influence of microphone repartition in the IMES results when the measurement data are obtained with FEM software.

3.2.2 FEM/IMES Simulation

This section deals with the influence of acoustic measurements in the detection and quantification of the vibration source. A new numerical methodology to identify the loads acting on the structure using FE method will be presented in this example. A more realistic test case will be then considered. The first step consists in subdividing a plane parallel to the plate with a distance e = 0.05 m, into nine areas, and placing a microphone in the middle of each area. In fact, the $n_{M_a} = 9$ acoustic measurement were distributed as shown in Fig. 13(a).

A color map of the estimated power repartition in the plate is drown in Fig. 13(b). From a first view, the highest value of power is estimated with a value equal to 0.8949 W/m^2. The next step consists in distributing the same number of microphones near the highest power surfaces with an equal distance $d_x = d_y = 0.09$ m (Fig. 14(a)).

As seen in this figure, a good input power prediction is observed. It should be noted that in Fig. 14(b), the source is correctly estimated for both localization and level.

Errors of the estimated power are summarized in Table 1. The results show that the amount of source information increases as the measurement point is so close from the source. Therefore, it is preferable that the distances between source and nearest measurement points are as short as possible. Moreover, it seems that choosing a good disposition of acoustic measurement is quite important to estimate the input force. Finally, this section confirms that the present method tends to estimate the input force in the structure for a few number of acoustic measurements, and can be applied for industrial problems, such as aeronautics and automotive industry.

https://doi.org/10.1017/jmech.2017.24 Published online by Cambridge University Press

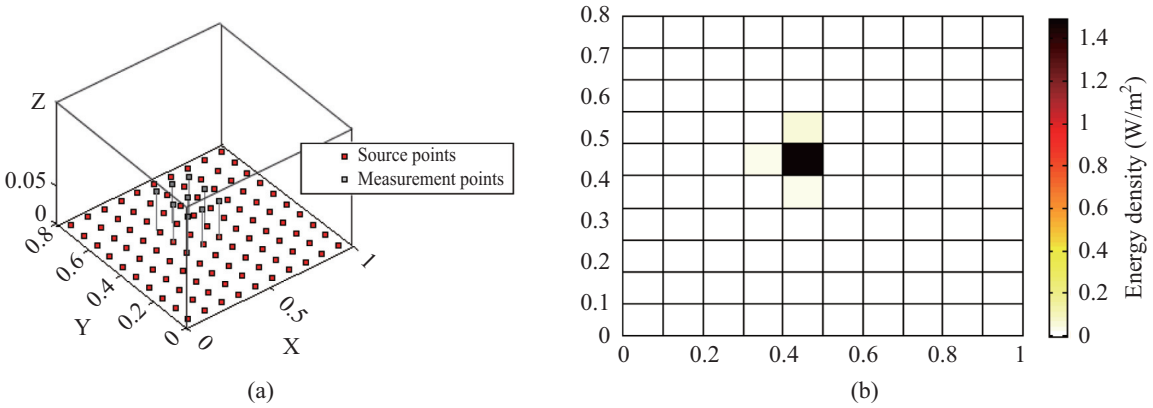


Fig. 14 FEM/IMES Simulation for $d_x = d_y = 0.09$ m.

Table 1 Estimated power error.

FEM/IMES Simulation	$d_x = 0.33$ m $d_y = 0.26$ m	$d_x = d_y = 0.09$ m
Error (%)	42.3	3.44

4. CONCLUSIONS

In this paper, numerical results are presented in order to localize the vibration source from acoustic measurement. The new IMES formulation based predictive tool has been first developed. Several test cases involving different measurement points and external forces were considered. The inverse solutions were compared to results given by the direct MES and FEM simulations. The obtained results confirm that the proposed approach accurately estimates the excitation force with a low density of measurement points. In the future works, the IMES could be developed to identify the acoustic sources. In other words, the identification of acoustic sources from structural measurements of energy density field using IMES method is currently being investigated.

ACKNOWLEDGEMENTS

This work has been funded by the Tunisian/French research cooperation program within the research project entitled "Optimization of sound packets by energetic aproach".

REFERENCES

1. Wang, Y. Q., Huang, X. B. and Li, J., "Hydroelastic Dynamic Analysis of Axially Moving Plates in Continuous Hot-Dip Galvanizing Process," *International Journal of Mechanical Sciences*, **110**, pp. 201-216 (2016).
2. Wang, Y. Q., Xue, S. W., Huang, X. B. and Du, W., "Vibrations of Axially Moving Vertical Rectangular Plates in Contact with Fluid," *International Journal of Structural Stability and Dynamics*, **16**, 1450092 (2016).
3. Wang, Y., Du, W., Huang, X. and Xue, S., "Study on the Dynamic Behavior of Axially Moving Rectangular Plates Partially Submersed in Fluid," A*cta Mechanica Solida Sinica*, **28**, pp. 706-721 (2015).
4. Wang, Y. Q., Guo, X. H., Sun, Z. and Li, J., "Stability and Dynamics of Axially Moving Unidirectional Plates Partially Immersed in a Liquid," *International Journal of Structural Stability and Dynamics*, **14**, 1450010 (2014).
5. Pezerat, C. and Guyader, J. L., "Identification of Vibration Sources," *Applied Acoustics*, **61**, pp. 309-324 (2000).
6. Pezerat, C. and Guyader, J. L., "Force Analysis Technique Reconstruction of Force Distribution on Plates," *Acoustica united with Acta Acustica*, **86**, pp. 322-332 (2000).
7. Pezerat, C. and Guyader, J. L., "Two Inverse Methods for Localization of External Sources Exciting a Beam," *Acta Acustica*, **3**, pp. 1-10 (1995).
8. Pezerat, C. and Guyader, J. L., "Force Analysis Technique: Reconstruction of Force Distribution on Plates," *Acta Acustica*, **86**, pp. 322-332 (2000).
9. Djamaa, M. C., Ouelaa, N., Pezerat, C. and Guyader, J. L., "Reconstruction of a Distributed Force Applied on a Thin Cylindrical Shell by an Inverse Method and Spatial Filtering," *Journal of Sound and Vibration*, **301**, pp. 560-575 (2007).
10. Williams, E. G., Maynard, J. D. and Skudrzyk, E., "Sound Source Reconstructions Using a Microphone Array," *Journal of the Acoustical Society of America*, **68**, pp. 340-344 (1980).

https://doi.org/10.1017/jmech.2017.24 Published online by Cambridge University Press

11. Maynard, J. D., Williams, E. G. and Lee, Y., "Near-Field Acoustic Holography: I. Theory of Generalized Holography and the Development of NHA," *Journal of the Acoustical Society of America*, **78**, pp. 1395-1413 (1985).
12. Pezerat, C., Leclère, Q., Totaro, N. and Pachebat, M., "Identification of Vibration Excitations from Acoustic Measurements Using Near Field Acoustic Holography and the Force Analysis Technique," *Journal of Sound and Vibration*, **326**, pp. 540-556 (2009).
13. Djamaa, M. C., Ouelaa, N., Pezerat, C. and Guyader, J. L., "Sound Source Localization by an Inverse Method Using the Measured Dynamic Response of a Cylinder," *Applied Acoustics*, **88**, pp. 22-29 (2015).
14. Ma, C. K., Chang, J. M. and Lin, D. C., "Input Forces Estimation of Beam Structures by an Inverse Method," *Journal of Sound and Vibration*, **259**, pp. 387-407 (2003).
15. Ji, C. C. and Liang, C., "A Study on an Estimation Method for Applied Force on the Rod," *Computer Methods in Applied Mechanics and Engineering*, **190**, pp. 1209-1220 (2000).
16. Liu, J. J., Ma, C. K., Kung, I. C. and Lin, D. C., "Input Force Estimation of a Cantilever Plate by Using a System Identification Technique," *Computer Methods in Applied Mechanics and Engineering*, **190**, pp. 1309-1322 (2000).
17. Baklouti, A., Antunes, J., Debut, V., Fakhkakh, T. and Haddar, M., "An Effective Method for the Identification of Support Features in Multi-Supported Systems," *In Advances in Acoustics and Vibration, Springer International Publishing*, pp. 301-312 (2017).
18. Lyon, R. H. and Dejong, R. G., "Theory and Application of Statical Energy Analysis," *Butterworth-Heineman*, Oxford (1995).
19. Nefske, D. J. and Sung, S. H., "Power Flow Finite Element Analysis of Dynamic Systems: Basic Theory and Application to Beams," *Journal of Vibration, Acoustics, Stress, and Reliability in Design*, **111**, pp. 94-100 (1987).
20. Wohlever, J. C. and Bernhard, R. J., "Mechanical Energy Flow Models of Rods and Beams," *Journal of Sound and Vibration*, **153**, pp. 1-19 (1992).
21. Bouthier, O. M. and Bernhard, R. J., "Simple Models of Energy Flow in Vibrating Membranes," *Journal of Sound and Vibration*, **182**, pp. 129-147 (1995).
22. Lase, Y., Ichchou, M. N. and Jezequel, L., "Energy Flow Analysis of Bars and Beams: Theoretical Formulations," *Journal of Sound and Vibration*, **192**, pp. 281-305 (1996).
23. Ichchou, M. N. and Jezequel, L., "Letter to the Editor: Comments on Simple Models of the Energy Flow in Vibrating Membranes and on Simple Models of the Energetics of Transversely Vibrating Plates," *Journal of Sound and Vibration*, **195**, pp. 679-685 (1996).
24. Ichchou, M. N., Le Bot, A. and Jezequel, L., "A Transient Local Energy Approach as an Alternative to Transient SEA: Wave and Telegraph Equations," *Journal of Sound and Vibration*, **246**, pp. 829-840 (2001).
25. Hardy, P., Ichchou, M., Jezequel, L. and Trentin, D., "A Hybrid Local Energy Formulation for Plates Mid-Frequency Flexural Vibrations," *European Journal of Mechanics - A/Solids*, **28**, pp. 121-130 (2009).
26. Besset, S., Ichchou, M. N. and Jezequel, L., "A Coupled BEM and Energy Flow Method for Mid-High Frequency Internal Acoustic," *Journal of Computational Acoustic*, **18**, pp. 69-85 (2010).
27. Cotoni, V., Le Bot, A. and Jezequel, L., "High Frequency Radiation of L-Shaped Plates by a Local Energy Flow Approach," *Journal of Sound and Vibration*, **250**, pp. 431-444 (2002).
28. Chachoub, M. A., Basset, S. and Ichchou, M. N., "Structural Sources Identification through an Inverse Mid-High Frequency Energy Method," *Mechanical Systems and Signal Processing*, **25**, pp. 2948-2961 (2011).
29. Chachoub, M. A., Basset, S. and Ichchou, M. N., "Identification of Acoustic Sources through an Inverse Energy Method," *Inverse Problems in Science and Engineering*, **19**, pp. 903-919 (2011).
30. Samet, A. *et al*., "Vibration Sources Identification in Coupled Thin Plates through an Inverse Energy Method," *Applied Acoustic*, http://doi.org/10.1016/j.apacoust.2016.12.001 (2017).
31. Ohayonand, R. Soize, C., *Structural Acoustics and Vibration: Mechanical Models, Variational Formulations and Discretization*, Academic Press, San Diego (1997).
32. Crighton, D. G., "Acoustic Edge Scattering of Elastic Surface Waves," *Journal of Sound and Vibration*, **22**, pp. 25-32 (1972).

(Manuscript received October 15, 2016, accepted for publication March 3, 2017.)

https://doi.org/10.1017/jmech.2017.24 Published online by Cambridge University Press